Considerations of a Double-Wall Cooling Design to Reduce Sand Blockage

Camron C. Land
Department of Mechanical Engineering,
Virginia Polytechnic Institute and State University,
Blacksburg, VA 24061

Chris Joe
Pratt and Whitney,
United Technologies Corporation,
East Hartford, CT 06108

Karen A. Thole
Department of Mechanical and Nuclear Engineering,
Pennsylvania State University,
University Park, PA 16803

Gas turbine engines use innovative cooling techniques to keep metal temperatures down while pushing the main gas temperature as high as possible. Cooling technologies such as film-cooling and impingement-cooling are generally used to reduce metal temperatures of the various components in the combustor and turbine sections. As cooling passages become more complicated, ingested particles can block these passages and greatly reduce the life of hot section components. This study investigates a double-walled cooling geometry with impingement- and film-cooling. A number of parameters were simulated to investigate the success of using impingement jets to reduce the size of particles in the cooling passages. Pressure ratios typically ranged between those used for combustor liner cooling and for blade outer air seal cooling whereby both these locations typically use double-walled liners. The results obtained in this study are applicable to more intricate geometries where the need to promote particle breakup exists. Results indicated that ingested sand had a large distribution of particle sizes where particles greater than 150 μm are primarily responsible for blocking the cooling passages. Results also showed that the blockage from these large particles was significantly influenced and can be significantly reduced by controlling the spacing between the film-cooling and impingement-cooling plates. [DOI: 10.1115/1.3153308]

1 Introduction

Gas turbine engines installed on aircraft are increasingly exposed to environments containing fine particles such as sand, ash, and dirt. When these fine particles are ingested into the engine, they can cause many problems at various locations within the engine. Most damage occurs during takeoff and landing at which time large amounts of particles can be ingested over short periods of time when engines are running at or near full power. Sand and other particles on the runway can be entrained into the inlet supplying the engine with its flow. Hamed et al. [1] reported that the formation of an unsteady vortex in front of the engine intake on the runway can entrain sand, dust, ice, and other particles into the engine. The possibility also exists for particles to be ingested at cruising altitude, which was further investigated in studies performed by Kim et al. [2] on aircraft flying through volcanic dust clouds.

Cooling air that flows through parts in the hot section of the turbine engine originates from the last stage of the compressor. The compressor bleed air is used to keep metal temperatures at acceptable levels in the combustor liner, turbine vanes, turbine blades, and turbine blade outer air seals. Common cooling geometries seen in these parts employ both internal convection, such as impingement-cooling, and external film-cooling. The issue is compounded by the fact that particles, such as sand, present in the compressor bleed air can block these cooling passages and holes leading to decreased part life.

Previous studies by Dunn et al. [3,4] and Batcho et al. [5] have indicated that the effects of particle ingestion in an engine include compressor erosion, deposition of materials on hot section components, blockage of combustor fuel nozzles, and blockage of cooling holes. The study reported in this document focuses on how sand can block the cooling passages and holes in a double-walled geometry. A double-walled geometry can be found in a gas turbine in several locations including a combustor liner, turbine blade outer air seal, and inside airfoils.

Similar to the investigation reported by Walsh et al. [6], this study quantified the blockage due to sand ingestion by measuring the reduction in coolant flow through an array of cooling holes at a given pressure ratio. While the study here reports data for a double-walled geometry at room temperature conditions, Walsh et al. [6] investigated the effects of temperature on the blocking of film-cooling holes placed in a single wall coupon with film-cooling holes. Walsh et al. [6] found that when metal temperatures increased from 882 to 992°C, there was a minimal increase in flow blockages. When metal temperatures increased from 992 to 1038°C, however, a 2% increase in the flow blockage from 5.7% to 7.7% resulted.

A double-walled coupon was used in this study to simulate commonly found cooling geometries. The coupon used had an inlet plate with an array of impingement holes and an exit plate with an array of film-cooling holes. The primary research objective was to determine whether impingement could be beneficial for breaking up particles in cooling passages thereby minimizing sand blockage in the film-cooling holes. The results presented can be expanded to include guidelines for cooling geometries whereby impingement flow can promote particle fragmentation. Many conditions were investigated to confirm the effects of impinging flows including pressure ratio, sand amount, sand distribution, plate spacing, and hole alignment. This paper includes a description of the experimental facility and methodology, sand characterization, and finally the results of the testing performed to determine the amount of flow blockage due to sand for a range of conditions.

2 Past Relevant Studies

Particles in the main gas path can block cooling holes on the external side due to deposition. This deposition can lead to severe increases in heat transfer coefficients as well as decreased levels of film-coolant. On the internal side of the turbine components, particles can also adhere to the inner walls that lead to flow blockages of the channels as well as film-cooling holes. There is a range

Contributed by the International Gas Turbine Institute of ASME for publication in the JOURNAL OF TURBOMACHINERY. Manuscript received March 3, 2009; final manuscript received March 4, 2009; published online March 25, 2010. Review conducted by David Wisler. Paper presented at the ASME Turbo Expo 2008: Land, Sea, and Air (GT2008), Berlin, Germany, June 9–13, 2008.

of influences that can be considered when investigating the blockages of sand particles in coolant channels. For example, particle fragmentation can occur when particles flow through the engine and impact surfaces, which would lead to a favorable result in terms of reduced blockages. Moreover, the ratio of the flow velocity to the particle size and density, namely, given as the Stokes number, can also influence whether the particle is convected by the flow or drops out of the flow and deposits onto the surfaces.

Several studies have been performed that have examined plugging of cooling holes. Hussein and Tabakoff [7] computationally simulated flows through a turbine that showed the number of particle impacts increased with increasing particle size. They observed that the particles flowing through the main gas path of an axial-flow turbine were reflected from the blunt leading edges of the rotor blade and the nozzle guide vane trailing edge before finally passing through the rotor. They also reported particles being affected by centrifugal forces that convected the particles toward the outer casing. The centrifugal effect was in agreement with studies by Kim et al. [2] who found that lighter particles tend to follow the flow while heavier particles tend to be centrifuged. They conducted experimental tests on volcanic ash ingestion in two different hot section test systems consisting of a combustor and a set of nozzle guide vanes. Kim et al. [2] also found that the showerhead cooling holes located at the leading edge of turbine vanes plugged with dust, which resulted in a decrease in film-cooling effectiveness. Batcho et al. [5] observed partial or complete blockage of vane and blade cooling holes in aircraft engines that had been flown through dust clouds. Such plugging results in metal temperatures rising above their melting temperature leading to hardware damage.

Since the cooling air for the combustor liner and turbine is bled from the last stage of the compressor, particles are continuously interacting with various engine component surfaces. This interaction can cause the particles to become smaller due to the impingement forces as the particles progress through the engine. Dunn et al. [3] performed studies to determine whether there is a significant breakup of dust as it moves through the compressor of a gas turbine engine. The level of fragmentation taking place in the fan and compressor that was deduced from collecting particles downstream of the bypass and in the environmental control system was also investigated. Note that the environmental control system bleeds air from the last stage of the compressor to provide air, temperature control, and pressurization for the passengers and crew. As such, the control system air has a similar concentration of particles to that of the bleed air for cooling the combustor and turbine components. Dunn et al. [3] reported in the study that both the particles collected from the fan bypass air and from the environmental control system were nominally the same size, but significantly smaller in size than the particles that were ingested into the engine. This finding led them to believe that most of the fragmentation occurred in the first few fan and compressor stages. Particle breakup was also observed in studies by Mann and Warnes [8] and Tilly and Sage [9], the latter of which confirmed the fragmentation behavior of irregular quartz particles during impact.

It is important to make use of what is already known for the heat transfer of impingement jets since this helps in better understanding how the sand may be reacting in a double-walled liner. This knowledge also helps us to determine whether what we are suggesting, namely, utilizing jet impingement for breaking up particles, will negatively influence the expected heat transfer from jet impingement. The particles that pass through the fan and compressor stages can be further broken down into smaller pieces using cooling methods that promote fragmentation. One of these methods for cooling in a turbine engine is jet impingement. According to Uysal et al. [10], the performance of impingement-cooling is influenced by flow in the cross direction. The level of crossflow decreases as the spacing between the jet and impinging surfaces increases. The impingement jet, however, becomes weaker as the spacing increases, which also reduces the desired

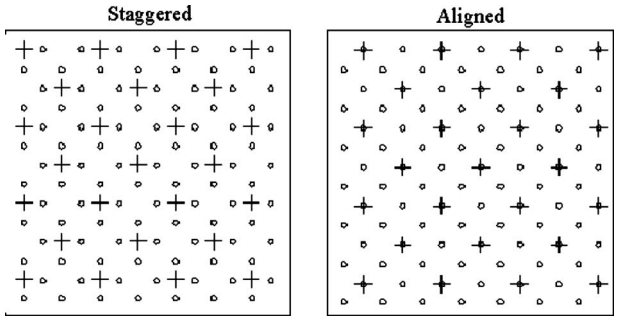

Fig. 1 The alignment of the impingement jets with respect to the film-cooling jets (+=impingement jets and deg=film-cooling jets)

effect of high heat transfer coefficients. Therefore, a tradeoff exists between wall spacing and cooling jet performance. According to Florschuetz et al. [11] and Van Treuren et al. [12], for very narrow distances between the impingement exit and impinging surface, $(S/D_J \sim 1)$, crossflow increases the heat transfer as it convects more coolant from upstream. Uysal et al. [10] found the differences in heat transfer among cases with the wall spacing to hole diameter values between 0.73 and 2.2 to be small, and there was only slightly better heat transfer performance observed when $S/D_J=1.5$. When the wall spacing is narrow, the jet failed to develop a sufficient level of turbulence for heat transfer enhancement at the impingement location. On the other hand, jet flow with very large wall spacing dissipates excessively and does not penetrate the crossflow, which results in lower heat transfer at the impingement surface.

Ingested sand passes through many areas in an engine with the particle size varying as a result of surface impacts. The sand also blocks cooling passages both internally from the coolant bleed air and externally by deposition from the main gas path. The focus of this study is on reducing sand blockage within gas turbine engine hardware. Promoting particle breakup may achieve this result by altering cooling geometries to increase high velocity surface impacts. This study will provide engine designers knowledge about the factors affecting sand fragmentation and blockage to allow better hardware designs to be developed.

3 Experimental Facility and Methodology

To characterize the flow blockage in the double-walled coupon illustrated in Fig. 1, the pressure ratio and cooling air flow rate were measured. The pressure ratio refers to the ratio of the supply coolant pressure to the exit static pressure, as shown in

$$\mathrm{PR} = \frac{P_{0C}}{P_\infty} \tag{1}$$

The supply coolant pressure was measured upstream of the double-walled coupon while the exit static pressure, the atmospheric pressure in the test laboratory, was measured downstream of the coupon. The coolant flow rate is reported in terms of a flow parameter defined by Hill and Peterson [13] as

$$\mathrm{FP} = \frac{4\dot{m}\sqrt{RT_{0C}}}{\pi P_\infty N D^2} \tag{2}$$

The supply coolant temperature was measured upstream of the laminar flow element and verified to be at the same total temperature measured upstream of the double-walled coupon. If a cooling geometry was altered, the flow parameter changed. Any blockage in the double-walled test coupon caused a reduction in flow parameter. The comparison of this reduced flow parameter to the flow parameter with no blockage gave the results presented in this paper.

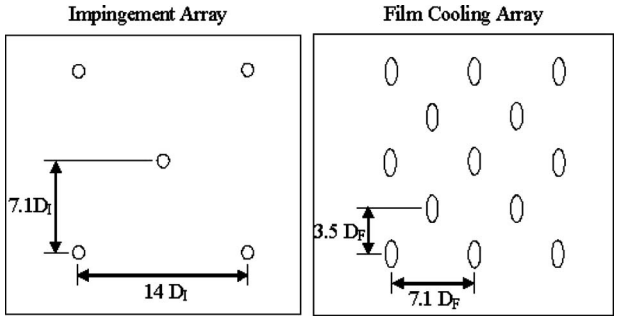

Fig. 2 The hole layout for the impingement- and film-cooling arrays

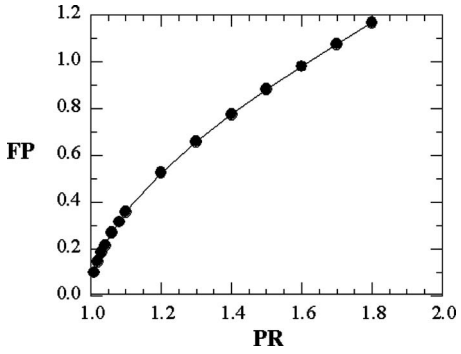

Fig. 4 Baseline flow parameter for all tests using a clean test coupon

The combination of impingement-cooling and film-cooling is a common cooling technique found in the combustor liner and the turbine blade outer air seal. Figure 1 shows the alignment of the impingement holes with respect to the film-cooling holes for two different configurations that were used for the test coupon. For most of the tests in this study, the impingement jets were staggered with respect to the film-cooling jets. A few tests, however, were conducted with the impingement- and film-cooling holes aligned to determine if using impingement was advantageous in breaking up particles.

The test coupon consisted of two plates separated by a spacer plate that fixed the distance between the impingement- and film-cooling holes. Figure 2 shows the hole arrangement on both the impingement- and film-cooling plates. The impingement plate contained 25 impingement holes with a diameter of 0.51 mm. The holes were made using electrical discharge machining (EDM) at 90 deg with respect to the surface. The impingement plate was 1.27 mm thick giving a hole length to diameter ratio of $L/D_I = 2.5$. The spacer plates that were used had thicknesses ranging from 0.79 mm to 3.18 mm, which allowed the spacing to diameter ratio to vary from $S/D_I = 1.56$ to 6.25. The second plate contained 98 film-cooling holes made using EDM with a diameter of 0.51 mm. The holes were angled at 30 deg with respect to the surface. The film-cooling plate was 0.89 mm thick giving a ratio of $L/D_F = 2$.

Figure 3 illustrates the test apparatus for supplying air and sand to the test coupon as well as the location of the measurements made. The coolant air was supplied to the test coupon at an elevated pressure from a compressed air line at room temperature. The pressure was regulated between 2 kPa and 73 kPa. The amount of coolant was controlled by a pressure regulator and a precision control valve that both contained screens to filter any particles. The coolant flow was measured with a laminar flow element (LFE) having a maximum capacity of 0.0014 m^3/s. The laminar flow element was positioned between two pieces of pipe

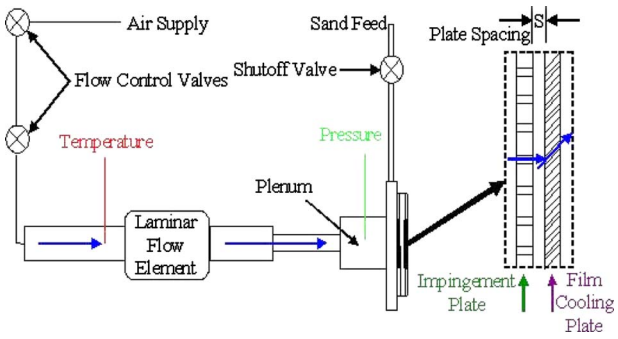

Fig. 3 Test apparatus for supplying the sand-air mixture to the test coupon

that extended approximately ten diameters upstream and ten diameters downstream of the LFE to ensure that fully developed flow conditions were present.

The instrumentation used to conduct the experiments in this study included pressure transducers, thermocouples, a LFE, and a precision scale to weigh the sand particles. A Type *K* nickel-chrome sheathed thermocouple probe was used to monitor the coolant temperature. The area ratio of the plenum cross section to the impingement holes was sufficiently large (144:1), and therefore the pressure measurements taken inside the plenum, which was upstream of the impingement plate, were treated as the total coolant supply pressure.

Prior to performing tests with injected sand particles, baseline measurements were made to determine the flow parameter and pressure ratio under clean conditions. These baseline measurements covered the full range of possible pressure ratios that were seen during testing with sand particles. Figure 4 shows the baseline flow parameter versus pressure ratio for the test coupon. Testing verified that the flow parameter was the same for all spacing and hole alignments.

Deposition within the engine is most likely to occur over a longer period of time than the method used in this study in which a slug of sand was introduced to the part. To assure realistic results, several tests were performed to determine if a slug of a given sand amount has the same blocking characteristics as when the given sand amount was divided into portions. It was verified that the cumulative sand amount equaled that used for the single slug tests. Representative results of these comparison tests can be found in a companion paper [15]. The tests indicate an insensitivity to how the sand was introduced into the liner as both the cumulative and slug tests resulted in the same overall blockage.

For the sand injection tests, a small oven was used to first dry the sand at 150°C for a time period of at least 4 h to remove any laboratory humidity effects. Following this drying process, the coolant flow rate to the coupon was set using the precision control valves shown in Fig. 3. Having reached the desired pressure ratio, the flow parameter was determined and compared with the baseline flow parameter. If the flow did not match the expected flow, it was most likely that there was sand remaining in the coupon from the previous test. If the expected flow was not achieved, the coupon was disassembled and cleaned using compressed air or by passing a small wire through the cooling holes. This process was continued until the baseline flow parameter was achieved for the pressure ratio.

After successfully cleaning the coupon and setting the desired pressure ratio, the sand was removed from the oven, weighed, and loaded into the airtight section of pipe with the shutoff valve at the sand feed (refer to Fig. 3). The sand remained in the hot oven until immediately before each test, but it returned to room temperature prior to releasing it into the coupon for testing. The amount of sand selected to flow through the test coupon corresponded to the amount of sand needed to simulate flow blockage levels that oc-

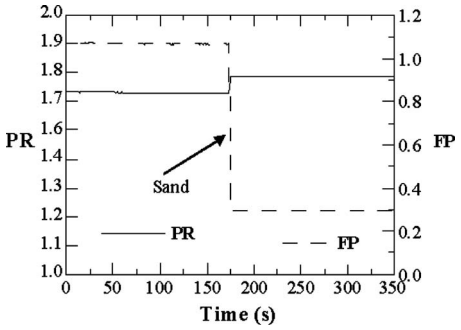

Fig. 5 Pressure ratio and flow parameter versus time (staggered, S/D_I=6.25, 0.35 g, $0<D_S<3800$ μm)

curred in actual engine components in studies by Walsh et al. [6]. With steady flow conditions achieved (Fig. 5), the feed valve was opened to introduce the sand into the coolant flow stream. The sand then flowed through the test coupon in a very short time period being on the order of a couple of seconds. The flow rate and pressure ratio were then again recorded. As a result of the sand injection, the rate of flow passing through the coupon decreased and the pressure upstream of the test coupon increased as shown in Fig. 5. Also seen in Fig. 5 was that after blockage was achieved, it remained steady over time. The reduction in flow parameter (RFP) was then calculated using

$$\mathrm{RFP} = \left.\frac{\mathrm{FP}_0 - \mathrm{FP}}{\mathrm{FP}_0}\right|_{\mathrm{PR}} \tag{3}$$

It is also interesting to note that testing indicated the same blockage results for the same cumulative sand amount. In other words, testing was done by dividing up the total amount of sand into three portions and comparing that with the total amount of sand for one test. The results from cumulatively adding the sand or by injecting the total amount of sand at one time resulted in the same blockage levels [14].

3.1 Uncertainty Analysis. For all of the results presented in this paper, three tests were conducted with the average of these three tests reported as the final value. A 25 case repeatability study conducted by Walsh et al. [6] showed that three tests conducted for each case considered resulted in repeatable results to within 7%. In addition, multiple investigators have performed these studies spanning over 1 year. Their results also indicate that an average of three tests resulted in good repeatability. Each data point presented by this study corresponds to an average of three independent tests. Figure 6 shows the baseline flow parameter with the three resulting flow parameters following the introduction of sand

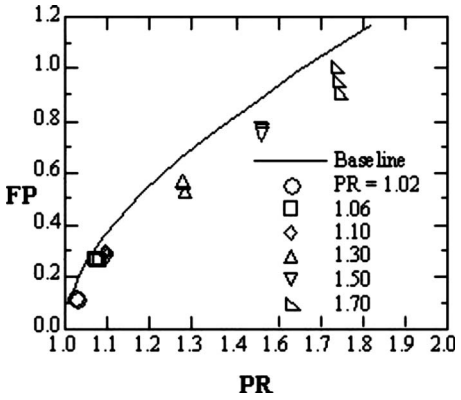

Fig. 6 Flow parameter baseline and repeated sand tests (staggered, S/D_I=3.13, 0.35 g, $0<D_S<3800$ μm)

Table 1 Parameter uncertainties

	Low RFP	High RFP	Low RFP	High RFP
PR	$1.02\pm0.122\%$	$1.10\pm0.114\%$	$1.71\pm0.0734\%$	$1.76\pm0.0711\%$
FP_0	$0.153\pm2.59\%$	$0.358\pm1.89\%$	$1.08\pm1.44\%$	$1.13\pm1.43\%$
FP	$0.143\pm2.70\%$	$0.0956\pm3.72\%$	$1.02\pm1.45\%$	$0.295\pm2.19\%$
RFP	$0.0690\pm50.7\%$	$0.733\pm1.52\%$	$0.0531\pm36.4\%$	$0.739\pm0.920\%$

for a set of tests. The uncertainty associated with the parameters discussed in this study was estimated using the partial derivative propagation of uncertainty method of Kline and McClintock [15]. The results of performing the uncertainty calculations are shown in Table 1.

The uncertainties were at a given pressure ratio for a low and high value of RFP. The pressure ratio uncertainties were relatively low and were dominated by the bias uncertainty of the pressure transducer detecting the plenum pressure upstream of the test coupon. The uncertainties of the flow parameter and reduction in flow parameter were heavily influenced by the bias uncertainty of the pressure transducer measuring the total pressure directly upstream of the laminar flow element. The uncertainty of the amount of sand injected into the flow was directly dependent on the accuracy of the scale used to weigh the sand. For most tests the amount of sand used was 0.35 ± 0.001 g. The higher the value of RFP was, the lower the percent uncertainty.

3.2 Sand Characterization. Many different types of sand were initially tested to determine the effects of sand on blockage in the double-walled test coupon. In the study by Walsh et al. [6], International Standards Organization (ISO) fine test dust and ISO coarse test dust were used to determine flow blockage in a leading edge coupon with an array of film-cooling holes having a diameter of 0.38 mm. Tests performed on the double-walled liner in the current study utilized the same sand from the Walsh et al. [6] study resulting in negligible blockage. The ISO fine sand contained no particles with a diameter over 150 μm, and the ISO coarse sand contained at most 2% of particles over 150 μm by volume.

The sand chosen for the current study was provided by the industry sponsor and was similar to the ISO sands with the exception of a few major differences. The ISO sands did not agglomerate as did the sand used for this study. The range of particles in our sand, including agglomerations, was larger than the range of particles in the ISO sands. Figure 7 shows the results of three different sand characterization methods used to determine the percentage of particles in a sample that are below a given sand diameter. With a small applied force, almost all particles over 150 μm could be broken down into smaller particles. Note that these studies used nonsieved and sieved sand samples whereby the sieved sand contained only particles over 150 μm. Tests were specifically conducted with sieved sand to determine the effects of larger particles on blockage.

A Horiba Partica LA-950 laser diffraction analyzer was originally used to characterize the sand, but difficulties emerged from this wet method because the method itself caused a breaking down of particles prior to analysis. The analyzer used a combination of liquid dispersant, circulation, and agitation to inspect the particles, which all caused the sand to reduce to a base size and was not consistent with what entered the test coupon.

The sand was also measured using newer technology in particle size analysis, which does not use liquid as the dispersing fluid. The new technology was released as an accessory for the Horiba Partica LA-950 called the powderjet dry feeder. The particles of interest were dropped through a similar measurement cell as the wet method using a vibratory feeder, which used air and a vacuum to disperse the sand. In the wet method, the liquid dispersant was assumed to cause the majority of the sand to break up, so the dry method was attempted to obtain a more accurate characterization.

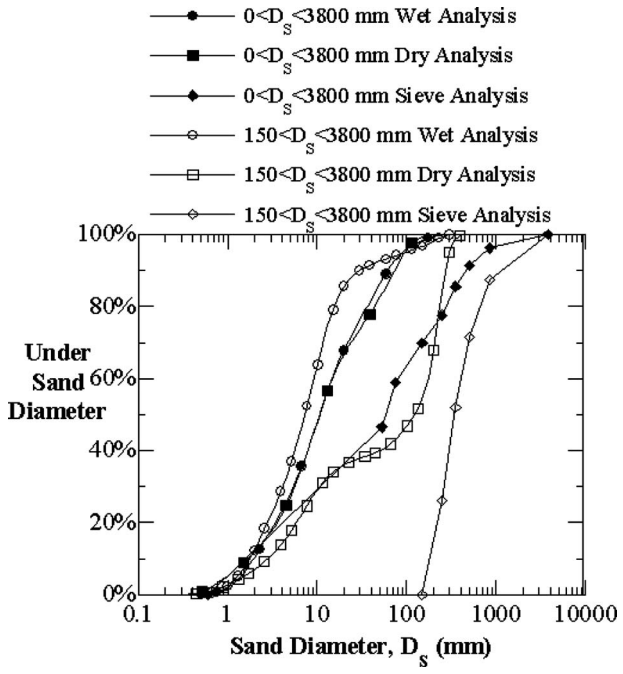

Fig. 7 Percentage of particles under size versus sand diameter for three measurement methods

Unfortunately, the dry method also resulted in the breakdown of particles, and the characterization again did not accurately describe the size of sand particles reaching the test coupon.

Finally, a simple sieve analysis was performed to accurately determine the range of sand particle diameters during testing. The sieve analyses gave the size distribution by using a range of sieves to separate the particles. The separated particles were then weighed and the fraction of particles for a particle diameter range was then calculated based on the weight of a particular sample size. The results of the sieve analysis are shown in Fig. 7 by percent of particles under the corresponding diameter. Sieves with mesh sizes ranging from 53 μm to 850 μm were stacked in descending order with the largest sieve at the top. Then a sample of sand was weighed and loaded into the top sieve in the stack. The stack was agitated until the sand grains remained in the sieve corresponding to the grains' sizes. The sand present in each sieve was then weighed as well as the sand that passed through all of the sieves. Using the total sample weight, a percentage was calculated from the amount of sand in a single sieve compared with the total. Particles as large as 3800 μm were measured with calipers. This sieve method provided what we believed to be the most accurate characterization of the sand distribution.

The chosen test sand is comprised primarily of crushed quartz [6]. The analysis of each of the sand samples agrees with the manufacturer's specification stating that it contains different phases of quartz (SiO_2) up to approximately 68–76%. The other major constituent is aluminum oxide (Al_2O_3) between 10% and 15%, with traces of iron oxide (Fe_2O_3), sodium silicate (Na_2O), lime (CaO), magnesium oxide (MgO), titanium dioxide (TiO_2), and potassium oxide (K_2O), in descending concentration.

4 Discussion of Results

The goal of this study was to determine an optimal wall spacing to minimize sand blockage in the double-walled test coupon. Many different parameters were investigated including sand amount (weight), sand size, wall spacing, hole alignment, and pressure ratio to determine their relative importance in affecting sand blockage. The results from performing this investigation are now discussed.

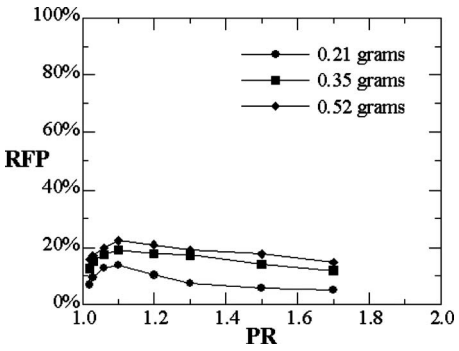

Fig. 8 Reduction in flow parameter for varying sand amounts (staggered, S/D_I=3.13, $0<D_S<3800$ μm)

4.1 Variation of Sand Amount. For the double-walled test coupon, varying amounts of nonsieved sand were injected into the coolant upstream of the test coupon at varying pressure ratios. Within a modern gas turbine engine, pressure ratios below 1.1 are typically available for injecting coolant through the combustor liner. Pressure ratios above 1.1 are typically available for cooling the first stage turbine blades and outer air seals. Figure 8 shows the effect of varying the amount of sand for the case with a staggered hole alignment, a wall spacing of S/D_I=3.13, and nonsieved sand at the full range of pressure ratios. Based on testing with actual engine parts injected with various amounts of sand, low, medium, and high sand amounts by weight were selected. The sand amount range of 0.2–0.4 g produced blockage results closest to actual part tests performed in congruence with this study.

The results showed that the blockage increased for pressure ratios from 1.02 to 1.1 and then decreased for pressure ratios of 1.1–1.7. From examinations of the test coupon, blockage mostly occurred in the impingement holes for pressure ratios below 1.1 leading to the conclusion that the air flow was too low to carry the sand through the coupon and the impingement plate acted as a filter. At pressure ratios above 1.1, it is believed that the sand was entrained in the flow through the impingement holes and caused most of the blockage in the film-cooling holes. Increasing the pressure ratio increased the velocity of the impingement jets on the upstream side of the film-cooling plate and therefore promoted particle fragmentation, which led to lower reductions in flow parameter. Figure 9 indicates that the reduction in flow parameter increased for increasing sand amounts, which was expected. Having verified varying sand amounts, the medium sand amount (0.35 g) was injected for the remainder of the results.

4.2 Variation of Sand Diameter Distribution. Sand having different size distributions, achieved through filtering with a sieve,

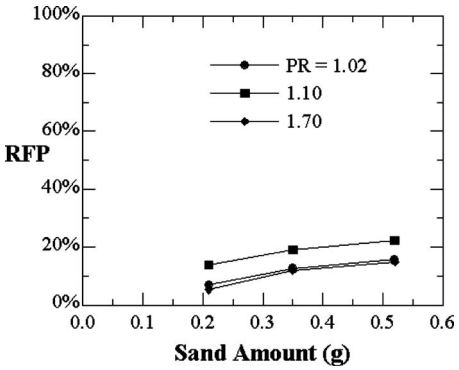

Fig. 9 Reduction in flow parameter for sand amounts (staggered, S/D_I=3.13, $0<D_S<3800$ μm)

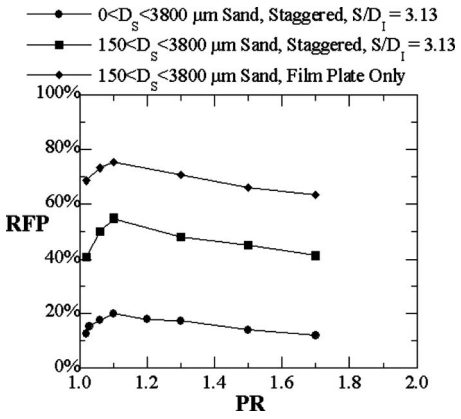

Fig. 10 Reduction in flow for different cases. Note that two samples were sieved (150–3800 μm) and the other was not (0–3800 μm).

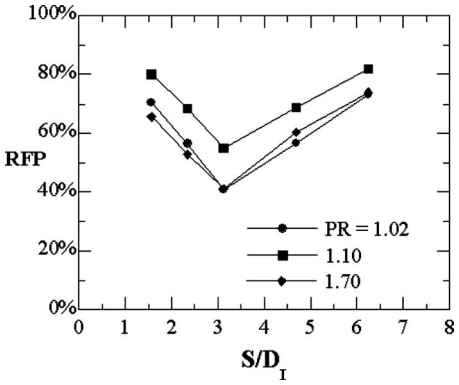

Fig. 12 Reduction in flow parameter for different plate spacings at different pressure ratios (staggered, 0.35 g, 150< D_S <3800 μm)

was injected into the coolant upstream of the test coupon at varying pressure ratios. Figure 10 shows the effect of varying the sand distribution using sieved (150–3800 μm) and nonsieved (0–3800 μm) sands. The nonsieved sand in Fig. 7 contained the full range of sand diameters. The sieved sand sample was produced by passing the sand through a sieve and contained only particles larger than 150 μm. The sieved sand sample caused blockage as high as 80%. The nonsieved sand contained a small percentage of particles above 150 μm in diameter, so there was some blockage with those sand samples. The blockage greatly increased from the sample that had only particles above 150 μm in diameter. For the remaining results presented in this paper, only the sand with particle diameters over 150 μm was used in testing. The dramatic increase in blockage led to focusing on the larger sand particles.

Also shown in Fig. 10 are the results from testing with only the film plate using sieved sand at the full range of pressure ratios. The impingement plate was removed for these tests to observe the effects of the sieved sand without impingement. The results showed that the reduction in flow parameter increased at all pressure ratios without the impingement plate, which indicates that impingement was beneficial and useful for breaking up particles.

4.3 Variation of Plate Spacing. Varying spacer thicknesses between the film and impingement plates were tested for different pressure ratios. Figure 11 shows the effect of varying S/D_I for the case with the staggered hole alignment, sand amount of 0.35 g, and sand with particle sizes of 150 μm and above at the full range of pressure ratios. As seen before, blockage increased for pressure ratios from 1.02 to 1.1 and then decreased for pressure ratios from 1.1 to 1.7. The S/D_I ratio of 3.13 performed considerably better than the others. The reasons for this reduced blockage at S/D_I=3.13 are because the crossflow for the small plate spacings disturbed the advantageous impingement velocities that promoted particle breakup. At large plate spacings, the decreased impingement velocities at the film-cooling plate due to jet spreading caused more blockage due to jets not penetrating to the film-cooling plate.

Figure 12 shows the same data as in Fig. 11 only plotted as a function of plate spacing at a given pressure ratio. A plate spacing existed that reduced the debilitating effects of crossflow and increased the beneficial effects of impingement velocity. Finding the balance between these two effects can also improve heat transfer although no heat transfer measurements were made in the course of this study. Figure 13 gives a picture comparison of the upstream side of the film-cooling plate at varying plate spacings. The pictures were taken for the case with a pressure ratio of 1.3, staggered hole alignment, sand amount of 0.35 g, and sieved sand containing particles above 150 μm. Less sand appeared on the film-cooling plate for an S/D_I of 3.13, which corresponded to the settings that produced the least reduction in flow parameter. The location of the impingement holes with respect to the film-cooling holes was illustrated by the absence of sand, indicated by dark spots, directly in the center of sets of four film-cooling holes. The reason for this is because of the impingement jets that are directing the sand away. The regions having the largest accumulations of sand, indicated by the light coloring in Fig. 13, occurred at spots farthest from the center of the impingement holes for the largest and smallest plate spacings. These results indicate weaker impingement jets for those plate spacings.

4.4 Variation of Hole Alignment. Varying hole alignments were analyzed for different pressure ratios and S/D_I as shown in

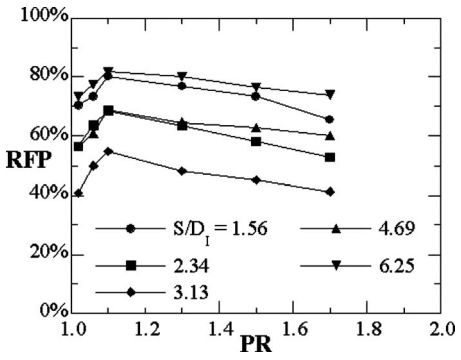

Fig. 11 Reduction in flow parameter for varying S/D_I (staggered, 0.35 g, 150< D_S <3800 μm)

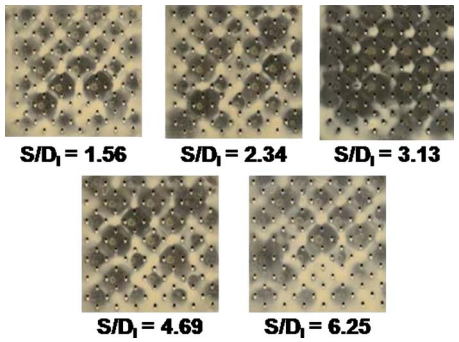

Fig. 13 Pictures taken on the upstream side of the film-cooling plate at varying S/D_I values (PR=1.3, 0.35 g, staggered, 150< D_S <3800 μm)

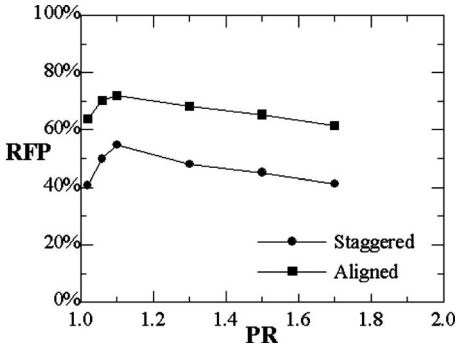

Fig. 14 Reduction in flow parameter for different alignments (S/D_I=3.13, 0.35 g, 150<D_S<3800 μm)

Fig. 14. Figure 14 shows the effect of varying the alignment of the holes in the impingement- and film-cooling plates for S/D_I =3.13, 0.35 g of sand, and sand with particle sizes of 150 μm and above, all at the full range of pressure ratios. The plate spacing of S/D_I=3.13 was chosen because it outperformed the other spacings tested. The blockage followed the same trend with respect to pressure ratio as observed in every case. The staggered arrangement of holes resulted in lower reduction in flow parameter than the aligned arrangement of holes. The staggered arrangement utilized impingement to reduce the size of the sand particles and reduce blockage.

Figure 15 shows the effect of varying hole alignment for the case with PR=1.3, 0.35 g of sand, and sand with particle sizes of 150 μm and above for a range of plate spacings. The effects of pressure ratio were thoroughly established by the previous results, so a single PR=1.3 was chosen to test the effects of hole alignment. Since the impingement holes were aligned with the film-cooling holes, the particle breakup due to impingement was decreased and the reduction in flow parameter increased. A similar trend as in the testing with the staggered arrangement was seen where the S/D_I=3.13 performed better for this range of tests. The data converge at low and high wall spacings because impingement was proven to be equally nonbeneficial in breaking up particles for these cases. These results are consistent with the explanation that at large plate spacings the impingement jets fail to penetrate to the film-cooling plate due to jet spreading and at small plate spacings the impingement jets fail to penetrate to the film-cooling plate due to crossflow. The location of the impingement holes with respect to the film-cooling holes influenced blockage less at these wall spacings.

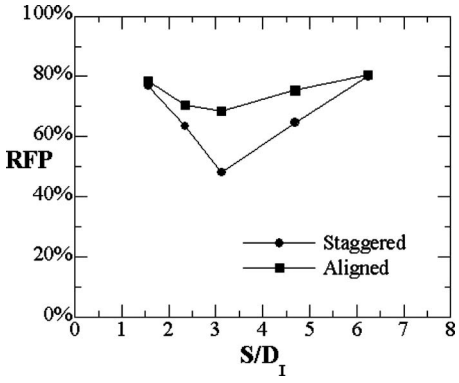

Fig. 15 Reduction in flow parameter for different plate spacings and alignments (PR=1.3, 0.35 g, 150<D_S<3800 μm)

5 Conclusions

Sand and dust on runways, during take-off conditions, and particles present in clouds, during in-flight conditions, are the primary sources of particle ingestion for aircraft turbine engines. Blockages from these particles in these cooling passages reduce the effectiveness of cooling by decreasing the coolant flow rate, and subsequently part life can be greatly reduced. In this study a double-walled coupon, representing a generic cooling geometry with impingement- and film-cooling holes, was tested to determine the effects of flow impingement on breaking up sand particles. Pressure ratio, sand amount, sand distribution, spacing of the double-wall, and hole alignment were all varied to test possible influences on particle fragmentation due to impingement flow. Greater blockages in the passages were always determined as the sand amount was increased to the coupon.

For all of the cases that were studied, blockage levels increased as the pressure ratio increased from 1.02 to 1.1. As the pressure ratio was increased beyond 1.1, the blockage levels decreased. Examination of the coupon after each test showed that below a pressure ratio of 1.1, most of the blockage occurred on the upstream side of the impingement plate. Sand particles were essentially filtered from the coolant stream by the impingement holes and were not carried through to the film-cooling holes. Above a pressure ratio of 1.1, sand was readily carried through the impingement holes with some blockage in the impingement holes, but most of the blockage occurred on the upstream side of the film-cooling plate.

By investigating the effects of particle diameters, the concentration of particles above 150 μm had a significant effect on blockage. Sand samples containing a higher concentration of 150 μm diameter caused higher blockage than sand samples that were nonsieved and contained a full range of particle diameters. The nonsieved sand, which contained a small percentage of particles with diameters greater than 150 μm, resulted in blockages that reduced the flow parameter by 5–25% while the sieved sand, containing only particles above 150 μm in diameter, resulted in blockages that reduced the flow parameter by 40–82%.

For all of the conditions considered, the spacing between the impingement and the film plates resulted in the least particle blockage for a spacing between the plates in the range of two to four impingement hole diameters. Visual inspection of the coupon revealed that less sand appeared on the upstream side of the film plate for the best plate spacing compared with the other spacings for a fixed sand amount, flow condition, and hole alignment. The reason for an optimal plate spacing can be best explained by considering that as the plate spacing is small, the crossflow between the holes adversely affects the impingement process thereby not allowing particle break-ups. At large plate spacings, the strength of the impingement jets was decreased also reducing particle fragmentation of the large particle sizes and agglomerations.

The alignment of the impingement holes with respect to the film-cooling holes confirmed the beneficial effects of impingement in breaking up large particles into smaller particles. The staggered arrangement, which allowed impingement on the back side of the film-cooling plate, showed less reduction in the flow parameter relative to the aligned arrangement, where the impingement- and film-cooling holes were aligned.

The results from these tests indicated that cooling geometries containing high velocity coolant jets impinging on a solid surface were helpful in breaking down particles into smaller particles. These smaller particles could then be carried through the cooling holes and exhausted into the main gas path without blocking the holes. In cooling geometries such as the double-walled liner used in this study, careful attention should be paid to the design if flow blockage due to sand ingestion is of concern.

Acknowledgment

The authors gratefully acknowledge the sponsors of this work, namely, United Technologies Corporation—Pratt & Whitney.

Nomenclature

D = diameter (m)
FP = flow parameter
L = cooling hole length (m)
$\dot{m}$ = mass flow (kg/s)
N = number of impingement holes
P = pressure (Pa)
PR = pressure ratio
R = gas constant for air (J/kg K)
S = wall spacing (m)
T = temperature (K)

Subscripts

F = film-cooling hole
I = impingement-cooling hole
S = sand
0 = baseline conditions with no sand
$0C$ = total property of the coolant
∞ = freestream conditions

References

[1] Hamed, A., Tabakoff, W., and Wenglarz, R., 2006, "Erosion and Deposition in Turbomachinery," J. Propul. Power, **22**(2), pp. 350–360.
[2] Kim, J., Dunn, M. G., Baran, A. J., Wade, D. P., and Tremba, E. L., 1993, "Deposition of Volcanic Materials in the Hot Sections of Two Gas Turbine Engines," ASME J. Eng. Gas Turbines Power, **115**, pp. 641–651.
[3] Dunn, M. G., Padova, C., and Adams, R. M., 1987, *Operation of Gas Turbine Engines in Dust-Laden Environments*, AGARD-Advanced Technology of Aero Engine Components, Paris, France.
[4] Dunn, M. G., Padova, C., Moller, J. C., and Adams, R. M., 1987, "Performance Deterioration of a Turbofan and a Turbojet Engine Upon Exposure to a Dust Environment," ASME J. Eng. Gas Turbines Power, **109**, pp. 336–343.
[5] Batcho, P. F., Moller, J. C., Padova, C., and Dunn, M. G., 1987, "Interpretation of Gas Turbine Response Due to Dust Ingestion," ASME J. Eng. Gas Turbines Power, **109**, pp. 344–352.
[6] Walsh, W. S., Thole, K. A., and Joe, C., 2006, "Effects of Sand Ingestion on the Blockage of Film-Cooling Holes," ASME Paper No. GT2006-90067.
[7] Hussein, M. F., and Tabakoff, W., 1974, "Computation and Plotting of Solid Particle Flow in Rotating Cascades," Comput. Fluids, **2**(1), pp. 1–15.
[8] Mann, D. L., and Warnes, G. D., 1994, "Future Directions in Helicopter Engine Protection System Configuration Turbines," 83rd Symposium, Propulsion and Energetic Panels of Erosion, Corrosion and Foreign Object Damage Effect in Gas Turbine 25-8.
[9] Tilly, G. P., and Sage, W., 1970, "The Interaction of Particles and Material Behaviour in Erosion Process," Wear, **16**, pp. 447–465.
[10] Uysal, U., Li, P.-W., Chyu, M. K., and Cunha, F. J., 2006, "Heat Transfer on Internal Surfaces of a Duct Subjected to Impingement of a Jet Array With Varying Jet Hole-Size and Spacing," ASME J. Turbomach., **128**, pp. 158–165.
[11] Florschuetz, L. W., Berry, R. A., and Metzger, D. E., 1980, "Periodic Streamwise Variations of Heat Transfer Coefficients for Inline and Staggered Arrays of Circular Jets With Crossflow of Spent Air," ASME J. Heat Transfer, **102**, pp. 132–137.
[12] Van Treuren, K. W., Wang, Z., Ireland, P. T., and Jones, T. V., 1993, "Detailed Measurements of Local Heat Transfer Coefficient and Adiabatic Wall Temperature Beneath and Array of Impinging Jets," ASME J. Turbomach., **116**, pp. 369–371.
[13] Hill, P., and Peterson, C., 1992, *Mechanics and Thermodynamics of Propulsion*, Addison-Wesley, Reading, MA.
[14] Cardwell, N. D., Thole, K. A., Burd, S. W., 2008, "Investigation of Sand Blocking Within Impingement and Film-Cooling Holes," ASME Paper No. GT2008-5135.
[15] Kline, S. J., and McClintock, F. A., 1953, "Describing Uncertainties in Single-Sample Experiments," Mech. Eng., **75**, pp. 3–8.